Published in final edited form as:
Epilepsia. 2002 October ; 43(10): 1210–1216.

Reduced Extrahippocampal NAA in Mesial Temporal Lobe Epilepsy

Susanne G. Mueller[*,‡], **Joyce Suhy**[*,‡], **Kenneth D. Laxer**[†], **Derek L. Flenniken**[*], **Jana Axelrad**[*], **Andres A. Capizzano**[*,‡,¶], and **Michael W. Weiner**[*,†,‡,§,‖]

[*]Department of Veterans Affairs (DVA) Medical Center, Magnetic Resonance Spectroscopy Unit, San Francisco, California, U.S.A.

[†]Deparment of Neurology, University of California San Francisco, Francisco, California, U.S.A.

[‡]Department of Radiology, University of California San Francisco, Francisco, California, U.S.A.

[§]Department of Medicine, University of California San Francisco, Francisco, California, U.S.A.

[‖]Department of Psychiatry, University of California San Francisco, San Francisco, California, U.S.A.

[¶]MRI Unit, Hospital Fernández, Buenos Aires, Argentina

Summary

Purpose—Structural and metabolic abnormalities in the hippocampal region in medial temporal lobe epilepsy (mTLE) are well described; less is known about extrahippocampal changes. This study was designed to characterize extrahippocampal metabolic abnormalities in mTLE with magnetic resonance spectroscopy in combination with tissue segmentation and volumetry of gray and white matter.

Methods—Multislice magnetic resonance spectroscopic imaging (^{1}H-MRSI) in combination with tissue segmentation was performed on 16 patients with mTLE and 12 age-matched healthy volunteers. The data were analyzed by using a regression-analysis model that estimated the metabolite concentrations in 100% cortical gray and 100% white matter in the frontal lobe and nonfrontal brain. The segmented image was used to calculate the fraction of gray and white matter in these regions.

Results—mTLE had significantly lower *N*-acetyl aspartate (NAA) in ipsi- and contralateral frontal gray ($p = 0.03$) and in ipsi- and contralateral nonfrontal white matter ($p = 0.008$) compared with controls. Although there were no associated volumetric deficits in frontal gray and white matter, ipsilateral nonfrontal gray matter ($p = 0.003$) was significantly smaller than that in controls.

Conclusions—mTLE is associated with extrahippocampal metabolic abnormalities and volumetric deficits, but these do not necessarily affect the same regions.

Keywords

Epilepsy; Spectroscopy; Extrahippocampal; Volumetry

In medial temporal lobe epilepsy (mTLE), the histopathologic hallmark of the primary epileptogenic region is mesio-temporal sclerosis, characterized by neuronal loss and reactive

Address correspondence and reprint requests to Dr. K.D. Laxer at Department of Neurology, University of California San Francisco, 400 Parnassus, San Francisco, CA 94143−0138, U.S.A. laxer@itsa.ucsf.edu.

astrogliosis in circumscribed areas of the hippocampus found in ~70% of the patients (1). However, seizures in mTLE are not confined to the me-dial temporal lobe structures but spread to other brain areas, especially the frontal lobes and the contralateral temporal lobe (2,3). Accordingly, volume abnormalities (4), neuropsychological deficits (5), alterations of cerebral glucose metabolism assessed by positron emission tomography (PET) (6-8), and benzodiazepine (BZD)-receptor binding (9) have demonstrated abnormalities beyond the temporal lobe in patients with mTLE. ^{1}H-magnetic resonance spectroscopy (^{1}H-MRS) can reliably detect the reduction of *N*-acetyl aspartate (NAA) associated with neuronal cell loss in the hippocampal region (10-14). Additionally, Li et al. (15) and Capizzano et al. (16) found reduced NAA in extrahippocampal regions. However, the NAA signal depends on the amount and the composition (gray/white matter ratio) of tissue present in the region from which the spectral data were obtained. Previously, a reduction of cortical gray matter volume, outside the temporal lobe, was reported (4). Because none of the previous MRS studies used tissue segmentation to account for varying contributions of gray and white matter, the reduced NAA could simply reflect an altered extrahippocampal gray matter content in mTLE. Therefore, the aim of this study was, by using tissue segmented MRI and multislice ^{1}H-MRS imaging, to determine if there are metabolic and/or volume abnormalities in extrahippocampal regions in mTLE and if they affect the same brain regions.

PATIENTS AND METHODS

Study population

The committee of human research at the University of California, San Francisco (UCSF) approved the study, and written informed consent was obtained from each subject according to the Declaration of Helsinki. The patients in this study were part of a larger population previously reported by Capizzano et al. (16). Sixteen patients (seven women and nine men) aged between 19 and 54 years (mean age, 37.7 ± 10.8 years) with nonlesional, drug-resistant mTLE were recruited from the Northern California Comprehensive Epilepsy Center, UCSF, where they underwent a presurgical exploration before anterior temporal lobe resection. Using video/EEG/telemetry (VET), MRI, and PET, the primary epileptogenic focus had been localized in the right mesio-temporal lobe (mTL) in five patients and in the left mTL in 11 patients. Table 1 displays the clinical characteristics of the patients. The control population consisted of 12 age-matched healthy volunteers (six women and six men), aged between 16 and 48 years (mean age, 30.8 ± 9.9 years).

Structural MRI acquisition and segmentation

The subjects were scanned on a 1.5-Tesla VISION MR system (Siemens Inc., Iselin, NJ, U.S.A.) by using a standard circularly polarized head coil. After scout images, the following MRI protocol was acquired: (a) T_1-weighted fast low angle shot (FLASH) in a tilted axial plane parallel to the long axis of the hippocampus, as defined in the sagittal scout images with TR/TE = 500/14 ms, flip angle 70°, slice thickness = 3 mm; (b) double spin-echo sequence (DSE) oriented along the anterior–posterior axis of the corpus callosum −10° with TR/TE1/TE2 = 2,500/20/80 ms timing, 1.0 × 1.4 mm^2 in-plane resolution, slice thickness = 3 mm; (c) volumetric magnetization-prepared rapid gradient echo (MPRAGE) oriented orthogonal to the T_1-weighted FLASH image plane with TR/TE/TI = 13.5/7/300 ms timing, 15° flip angle, 1.0 × 1.0 mm^2 in-plane resolution, slice thickness = 1.4 mm. Proton density and T_2-weighted images from DSE and T_1-weighted images from MPRAGE were used together for MRI tissue segmentation with software developed in this laboratory, described previously (17). First-pass segmentation of the whole-brain MRI data into the primary tissue categories of gray and white matter and CSF was performed by an automated procedure based on K-mean cluster analysis. Operator-assisted segmentation further classified white matter into normal white matter and white matter lesions, and gray matter into cortical gray matter and subcortical gray matter.

Finally, the hemispheric and rolandic fissures were manually delineated to mark the boundaries between right and left cerebral hemispheres and between the frontal lobes and the nonfrontal brain (cf. Fig. 1).

Volumes were calculated by summing pixels assigned to the different tissue categories (i.e., left and right frontal cortical gray matter, left and right frontal white matter, left and right nonfrontal cortical gray matter, and nonfrontal white matter) in the segmented image. To correct for different head sizes and thus allow comparison between different subjects, the absolute pixel counts for each region of a subject were expressed as percentage of the total intracranial pixel count (i.e., sum of cerebral pixels and pixels from cisternal and sulcal CSF) of this subject.

^{1}H-MRSI acquisition and spectral processing

Multislice ^{1}H-MRSI (TR/TE = 1,800/135 ms, 45-min total acquisition) was acquired from three 15-mm-thick slices aligned parallel to the DSE images (cf. Fig. 1), including slice-selective inversion-recovery (TI = 170 ms) to null the lipid signal and chemical shift selected (CHESS) water suppression. K-space sampling was accomplished with 36 × 36 circularly bounded phase-encoding steps across a 280 × 280-mm^2 field of view, yielding a nominal voxel size of ~0.9 ml. The lower slice (hippocampal slice) was placed covering the tail of the hippocampus, the middle slice (ventricular slice) right below the inferior aspect of the corpus callosum, and the upper slice (supraventricular slice) slightly above. The ^{1}H-MRSI data were zero-padded to 64 × 64 points in the spatial domain and 1,024 points in the spectral domain. Before Fourier reconstruction, the time-domain data were 2 Hz Gaussian filtered and deconvolved by using a Hamming filter to eliminate residual water resonances. Reduction of spurious resonances from extracranial lipids was accomplished by selective k-space extrapolation (18). A fully automated spectral fitting software package developed in this laboratory (19,20) was used to fit the data. Quality control was ensured by rejecting peaks that had a >12 Hz line width at half peak height or fits with residual sum squares that were outside the upper 95th percentile distribution of residuals from all fits. Typically no more than 10% of all voxels of the ventricular and supraventricular slice were rejected by these criteria, but ~80% of all voxels were rejected in the frontal and temporal lobe region of the hippocampal slice where the spectral quality was adversely affected by susceptibility artifacts typical for this region (cf. Fig. 2). Finally, the peak areas were corrected for receiver gain and expressed relative to the intensity of median ventricular CSF of each subject, as measured from the proton-density MRI.

MRI and ^{1}H-MRSI coanalysis

Tissue weights for each tissue type (i.e., cortical gray matter, subcortical gray matter, white matter, white matter lesions, CSF, and nonbrain tissue) in each MRSI voxel were determined with the data from the segmented MRIs. The segmented MRIs were aligned with the MRSI slices by using slice position and orientation information. The tissue weights were then computed by convolving each tissue map of the segmented MR images with the discrete transform of the MRSI spatial response function and MRSI slice profile, including corrections for chemical shift displacement and coil sensitivity (21). This determined the percentage of left and right frontal gray matter, frontal white matter, nonfrontal gray matter, and nonfrontal white matter in each MRSI voxel. To calculate the concentration of each metabolite in a voxel, its intensity in a voxel was expressed as a function of signal contribution from each tissue type and brain region and an error term representing the error from the estimation of the metabolite itself. The MRSI data from all three slices were fit by using a multiterm linear regression algorithm (SPLUS; Mathsoft, Inc., Seattle, WA, U.S.A.) to obtain estimates of the concentration of a metabolite in 100% cortical gray matter and in 100% white matter for each of the four brain regions. The concentrations are reported in arbitrary units.

Statistical analysis

Differences of metabolite concentrations in gray and white matter, brain regions, side (i.e., left/right for controls and ipsi-/contralateral in patients), and groups were tested by Kruskal–Wallis rank sum tests. A similar analysis was done to test for side differences in white and gray matter volume. Post hoc comparisons for all Kruskal–Wallis tests were done with multiple Wilcoxon tests corrected for multiple comparisons with Holm's test ($p < 0.05$).

RESULTS

Table 2 shows NAA, creatine/phosphocreatine (Cr), and choline compound (Cho) concentrations in cortical gray and white matter of both major brain regions. The differences of NAA, Cr, and Cho in the frontal lobe and the nonfrontal brain between white and gray matter for both groups are similar as previously reported from this laboratory (21). There were no significant effects for left and right sides in controls and for ipsi- and contralateral sides in patients. Therefore both hemispheres were combined for comparisons between patients and controls. NAA was lower in frontal gray matter (Wilcoxon signed rank: $Z = -2.13$; $p = 0.03$) of mTLE compared with controls. There were no differences between mTLE and controls for Cr and Cho in frontal gray or in frontal white matter. In nonfrontal brain, NAA was lower in white matter of mTLE compared with controls (Wilcoxon signed rank: $Z = -2.67$; $p = 0.008$). There were no further differences between both groups for this brain region.

Table 3 displays gray and white matter volumes of both major brain regions. There were no significant effects for left and right side in controls and for ipsi- and contralateral sides in patients. Therefore, both hemispheres were combined for comparisons between patients and controls. There was an effect for group in nonfrontal gray matter (Kruskal–Wallis: $\chi^2 = 11.09$; $df = 1$; $p = 0.0009$). After correction for multiple comparisons in mTLE, the mean ipsilateral percentage of nonfrontal gray matter was smaller than the corresponding mean in controls (Wilcoxon signed rank test: $Z = 2.29$; $p = 0.003$). There were no further white/gray matter volume differences between the two groups for the frontal lobe.

DISCUSSION

There were two major findings in this study: (a) NAA but not Cr and Cho was reduced in extrahippocampal white and gray matter bilaterally and symmetrically. In the frontal lobe, gray matter was affected; in nonfrontal brain, white matter was affected. (b) There was a significant reduction of gray matter in the nonfrontal brain ipsilateral to the epileptogenic focus compared with the corresponding region in controls. Taken together, these results provide additional evidence for structural and metabolic abnormalities beyond the primary epileptogenic region in mTLE. Furthermore, these structural and metabolic changes affect different brain regions.

The first major finding was a symmetrical and bilateral NAA reduction in the frontal lobe and nonfrontal brain. Regression analysis allowed us to detect abnormalities not only in cortical gray matter but also in white matter. In the frontal lobes, NAA was reduced in gray matter and also showed a tendency to be lower in frontal white matter ($p = 0.06$). In the nonfrontal brain, NAA was reduced in white matter but surprisingly was unchanged in gray matter. In analogy to the frontal lobe findings, it seems reasonable to expect also in the non-frontal brain an involvement of both tissue types. However, many voxels in the neocortical temporal gray matter were excluded because of poor spectral quality, thereby causing loss of spectral data from one of the most likely affected extrahippocampal brain regions in mTLE. The other regions were usually well represented by voxels from both tissue categories. Therefore, this apparent sparing of nonfrontal gray matter was probably an artifact caused by temporal lobe voxel exclusion. Because all extrahippocampal NAA reductions were bilateral and symmetrical in gray and white matter of both brain regions, they provided no information for

the lateralization of the primary epileptogenic hippocampus. The reduction of NAA in extrahippocampal brain regions in mTLE is in good agreement with two previous MRS studies (15,16) and also with several PET studies demonstrating not only mesio-temporal hypometabolism but also often temporo-neocortical and sometimes even frontal, occipital, parietal, and cerebellar metabolic disturbances (6,9,22,23).

Similar to the hippocampal findings in mTLE, NAA was the only metabolite reduced in extrahippocampal brain regions. Cr, thought to be a reliable marker of the brain energy metabolism, and Cho, which is considered to be a marker of membrane integrity, were both in the normal range. Therefore, the isolated reduction of NAA seems to be specific for the interictal state in mTLE. The exact function of NAA in the brain is still unknown. Because it is synthesized mainly in neuronal mitochondria and is localized in perikarya, axons, and dendrites of neurons in neurohistochemical studies (24,25), NAA is believed to be a marker of neuronal function and density. This seems to be true for the epileptogenic hippocampus in mTLE, in which NAA reductions are correlated to some degree with neuronal cell loss and neuronal function (26,27). However, recent studies have shown that NAA can be synthesized by oligodendrocytes as well (28), and maintaining a normal concentration of NAA makes neuronal–glial trafficking necessary because the degrading enzyme aspartoacylase exists only in glial cells (29-31). Furthermore, a recent case report describes a 3-year-old cognitively impaired child with complete absence of the NAA signal but only slightly abnormal MRI findings (32). Therefore, a reduction of NAA does not necessarily always indicate a loss of neurons but may as well be an indicator of some kind of neuronal–glial dysfunction. This may be especially true if there is no other evidence for neuronal loss, as in our study, in which the metabolite abnormalities were not associated with volume loss.

The reasons for the extrahippocampal NAA reductions are unknown, but there are several possible mechanisms. First, extrahippocampal NAA reductions are a marker of the unknown, underlying epileptogenic process in mTLE, which affects not only the primary epileptogenic region, but also the entire brain. This theory is supported by the fact that in the temporal lobes of patients with newly diagnosed mTLE, NAA is already reduced to the same degree as in patients with long-standing intractable mTLE (33,34). However, NAA reductions in the temporal lobes normalize after successful epilepsy surgery, l.e., after a symptomatic treatment most probably not correcting the underlying epileptogenic process (35). The second possible mechanism for extrahippocampal NAA reductions is that they are a consequence of repetitive seizures. Because seizures in mTLE are not confined to the primary epileptogenic region but spread to other brain regions as well, the same excitotoxic mechanisms leading to an NAA reduction in the hippocampus can induce an NAA reduction in regions involved in the seizure spread. Furthermore, the loss of efferent neurons in the hippocampus may lead to a deafferentation and changed function of neurons in other brain regions, that is associated with an NAA reduction (36). A third possible mechanism is that NAA reductions are caused by the treatment with antiepileptic drugs (AEDs) (37). Finally, it is possible that extrahippocampal NAA reductions are related to both the epileptogenic process and the effects of seizures and/or treatment.

The second major finding was a reduction of gray matter volume on the ipsilateral side in nonfrontal brain. Because most of the patients (11 of 16) had evidence for mesio-temporal lobe sclerosis, which is often associated with more widespread atrophy in the ipsilateral temporal lobe region (38-40), it seems reasonable to assume that the nonfrontal volume deficits in our study represented mostly a loss of ipsilateral temporal volume. In the frontal lobes, our volumetric studies showed no significantly different gray and white matter percentages in mTLE compared with controls. These findings contrast with the NAA reductions in the frontal lobe. Therefore the NAA reductions cannot be attributed to structural alterations. Furthermore, the fact that NAA was reduced in the frontal lobe in the absence of structural changes,

emphasizes the sensitivity of NAA. Our findings of no structural change in the frontal lobe are in good agreement with two previous studies using automated segmentation and voxel-by-voxel comparison (41,42), but contrast with findings of a third study that found bilateral reduced gray and white matter of the frontoparietal region in mTLE patients compared with healthy controls (4). However, differences between techniques, study populations, and anatomic definitions of the brain regions studied may explain these discrepancies.

We are aware that this study has limitations: (1) Because only the frontal lobe was defined for the study, we were not able to identify the affected lobes in the non-frontal brain. (2) Using regression analysis to calculate gray and white matter metabolite concentrations did not allow identification of specific voxels with reduced NAA. The spatial distribution of NAA reductions could give insight into the nature of the extrahippocampal involvement and even be of prognostic value for the outcome of epilepsy surgery.

In conclusion, mTLE is associated with extrahippocampal metabolic abnormalities similar to those found in the hippocampal region. Whereas the NAA reductions in the hippocampal region are more pronounced in the primary epileptogenic hippocampus and can thereby used to identify the seizure origin, extrahippocampal abnormalities are bilateral and symmetrical. Contrary to the hippocampus, where the NAA reductions are thought to reflect mainly neuronal cell loss and are often associated with hippocampal atrophy, extrahippocampal abnormalities are not associated with atrophy and therefore are probably secondary to a neuronal–glial dysfunction rather than to loss of neuronal cells.

Acknowledgment

This work was supported by NIH grant ROI-NS31966 (K.D.L)

S.G.M. was supported by a grant from the Swiss National Science Foundation.

REFERENCES

1. Babb, TL.; Brown, WJ. Pathological findings in epilepsy.. In: Engel, J., Jr, editor. Surgical treatment of the epilepsies. Raven Press; New York: 1987. p. 511-40.
2. Lieb JP, Dasheiff RM, Engel J. Role of the frontal lobes in the propagation of mesial temporal lobe seizures. Epilepsia 1991;32:822–37. [PubMed: 1743154]
3. Adam C, Saint-Hilaire JM, Richer F. Temporal and spatial characteristics of intracerebral seizure propagation: predictive value in surgery for temporal lobe epilepsy. Epilepsia 1994;35:1065–72. [PubMed: 7925153]
4. Marsh L, Morrell MJ, Shear PK, et al. Cortical and hippocampal volume deficits in temporal lobe epilepsy. Epilepsia 1997;38:576–87. [PubMed: 9184604]
5. Jokeit H, Seitz RJ, Markowitsch HJ, et al. Prefrontal asymmetric interictal glucose hypometabolism and cognitive impairment in patients with temporal lobe epilepsy. Brain 1997;120:2283–94. [PubMed: 9448582]
6. Henry TR, Mazziotta JC, Engel J. Interictal metabolic anatomy of mesial temporal lobe epilepsy. Arch Neurol 1993;50:582–9. [PubMed: 8503794]
7. Schlaug AS, Niemann H, Ebner A, et al. Topography of interictal glucose hypometabolism in unilateral mesiotemporal epilepsy. Neurology 1996;46:1422–30. [PubMed: 8628493]
8. Savic I, Altshuler L, Baxter L, et al. Pattern of interictal hypometabolism in PET scans with fluorodeoxyglucose F18 reflects prior seizure types in patients with mesial temporal lobe seizures. Arch Neurol 1997;54:129–36. [PubMed: 9041853]
9. Hammers A, Koepp MJ, Labbé C, et al. Neocortical abnormalities of [11C]-flumazenil PET in mesial temporal lobe epilepsy. Neurology 2001;56:897–906. [PubMed: 11294927]

10. Hugg JW, Laxer KD, Matson GB, et al. Neuron loss localizes human temporal lobe epilepsy by in vivo proton magnetic resonance spectroscopic imaging. Ann Neurol 1993;24:788–94. [PubMed: 8250527]
11. Ende GR, Laxer KD, Knowlton RC, et al. Temporal lobe epilepsy: bilateral hippocampal metabolite changes revealed at proton MR spectroscopic imaging. Radiology 1997;202:809–17. [PubMed: 9051038]
12. Cendes F, Caramanos Z, Andermann F, et al. Proton magnetic resonance spectroscopic imaging and magnetic resonance imaging volumetry in the lateralization of temporal lobe epilepsy: a series of 100 patients. Ann Neurol 1997;42:737–46. [PubMed: 9392573]
13. Kuzniecky R, Hugg JW, Hetherington H, et al. Relative utility of 1H spectroscopic imaging and hippocampal volumetry in the lateralization of mesial temporal lobe epilepsy. Neurology 1998;51:66–71. [PubMed: 9674780]
14. Chu WJ, Kuzniecky RI, Hugg JW, et al. Statistically driven identification of focal metabolic abnormalities in temporal lobe epilepsy with corrections for tissue heterogeneity using 1H spectroscopic imaging. Magn Reson Med 2000;43:359–67. [PubMed: 10725878]
15. Li ML, Cendes F, Andermann F, et al. Spatial extent of neuronal metabolic dysfunction measured by proton MR spectroscopic imaging in patients with localization related epilepsy. Epilepsia 2000;41:666–74. [PubMed: 10840397]
16. Capizzano AA, Vermathen P, Laxer KD, et al. Multi-slice 1HMRSI evaluation of nonlesional mesial temporal lobe epilepsy. AJNR Am J Neuroradiol. (in press)
17. Tanabe JL, Amend D, Schuff N, et al. Tissue segmentation of the brain in Alzheimer disease. AJNR Am J Neuroradiol 1997;18:115–23. [PubMed: 9010529]
18. Haupt CI, Schuff N, Weiner MW, et al. Removal of lipid artifacts in 1H spectroscopic imaging by data extrapolation. Magn Reson Med 1996;35:678–87. [PubMed: 8722819]
19. Maudsley AA, Lin E, Weiner MW. Spectroscopic imaging display and analysis. Magn Reson Imaging 1992;10:471–85. [PubMed: 1406098]
20. Soher BJ, Young K, Govindaraju V, et al. Automated spectral analysis, III: application to in vivo proton MR spectroscopy and spectroscopic imaging. Magn Reson Med 1998;40:822–31. [PubMed: 9840826]
21. Schuff N, Ezekiel F, Gamst AC, et al. Region and tissue differences of metabolites in normally aged brain using multislice 1H magnetic resonance spectroscopic imaging. Mag Reson Med 2001;45:899–907.
22. Savic I, Altshuler L, Passaro E, et al. Localized cerebellar hypometabolism in patients with complex partial seizures. Epilepsia 1996;37:781–7. [PubMed: 8764819]
23. Lamusuo S, Jutila L, Ylinen A, et al. [18F]FDG-PET reveals temporal hypometabolism in patients with temporal lobe epilepsy even when quantitative MRI and histopathological analysis show only mild hippocampal damage. Arch Neurol 2001;58:933–9. [PubMed: 11405808]
24. Simmons ML, Frondoza CG, Coyle JT. Immunocytochemical localization of *N*-acetyl-aspartate with monoclonal antibodies. Neuroscience 1991;45:37–45. [PubMed: 1754068]
25. Moffett HNR, Namboodiri MAA. Differential distribution of *N*-acetylaspartylglutamate and *N*-acteylaspartate immunoreactivi-ties in rat forebrain. J Neurocytol 1995;24:409–33. [PubMed: 7595659]
26. Ebisu T, Rooney WD, Graham SH, et al. *N*-Acetylaspartate as an in vivo marker of neuronal viability in kainate-induced status epilepticus: 1H magnetic resonance spectroscopic imaging. J Cereb Blood Flow Metab 1994;14:373–82. [PubMed: 8163579]
27. Sawrie SM, Martin RC, Gilliam FG, et al. Visual confrontation naming and hippocampal function: a neuronal network study using quantitative 1H magnetic resonance spectroscopy. Brain 2000;123:770–80. [PubMed: 10734008]
28. Bakhoo KK, Pearce D. In vitro expression of *N*-acetyl aspartate by oligodendrocytes: implications for proton magnetic resonance spectroscopy signal in vivo. J Neurochem 2000;74:254–62. [PubMed: 10617127]
29. Baslow MH. Functions of *N*-acetyl-l-aspartate and *N*-acetyl-l-aspartylglutamate in the vertebrate brain: role in glial cell-specific signaling. J Neurochem 2000;75:543–59.

30. Bakhoo KK, Craig TJ, Styles P. Developmental and regional distribution of aspartoacylase in rat brain tissue. J Neurochem 2001;79:211–20. [PubMed: 11595773]

31. Huang W, Wang H, Kekuda R, et al. Transport of N-acetyl-aspartate by the NA+ dependent high affinity dicarboxylate transporter NaDC3 and its relevance to the expression of the transporter in the brain. J Pharmacol Exp Ther 2000;295:392–403. [PubMed: 10992006]

32. Martin E, Capone A, Schneider J, et al. Absence of *N*-acetyl-aspartate in the human brain: Impact on neurospectroscopy? Ann Neurol 2001;49:518–21. [PubMed: 11310630]

33. Miller SP, Li LM, Cendes F, et al. Neuronal dysfunction in children with newly diagnosed temporal lobe epilepsy. Pediatr Neurol 2000;22:281–6. [PubMed: 10788744]

34. Li LM, Dubeau F, Andermann F, et al. Proton magnetic resonance spectroscopic imaging studies in patients with newly diagnosed partial epilepsy. Epilepsia 2000;41:825–31. [PubMed: 10897153]

35. Cendes F, Andermann F, Dubeau F, et al. Normalization of neuronal metabolic dysfunction after surgery for temporal lobe epilepsy: evidence from proton MR spectroscopic imaging. Neurology 1997;49:1525–33. [PubMed: 9409340]

36. Roffman JL, Lipska BK, Bertolino A, et al. Local and downstream effects of excitotoxic lesions in the rat medial prefrontal cortex on in vivo 1H-MRS signals. Neuropsychopharmacology 2000;22:430–9. [PubMed: 10700662]

37. O`Donnell T, Rotzinger S, Nakashima TT, et al. Chronic lithium and sodium valproate both decrease the concentration of myoinositol and increase the concentration of inositol monophosphates in rat brain. Brain Res 2000;880:84–91. [PubMed: 11032992]

38. Lee JW, Reutens DC, Dubeau F, et al. Morphometry in temporal lobe epilepsy. Magn Reson Imag 1995;13:1073–80.

39. Bernasconi N, Bernasconi A, Cramanos Z, et al. Morphometric MRI analysis of the parahippocampal region in temporal lobe epilepsy. Ann N Y Acad Sci 2000;911:495–500. [PubMed: 10911900]

40. Moran NF, Lemieux L, Kitchen ND, et al. Extrahippocampal temporal lobe atrophy in temporal lobe epilepsy and mesial temporal sclerosis. Brain 2001;124:167–75. [PubMed: 11133796]

41. Woermann FG, Free SL, Koepp MJ, et al. Voxel-by-voxel comparison of automatically segmented cerebral grey matter: a rater-independent comparison of structural MRI in patients with epilepsy. Neuroimage 1999;10:373–84. [PubMed: 10493896]

42. Woermann FG, Tebartz van Elst L, Koepp MJ, et al. Reduction of frontal neocortical grey matter associated with affective aggression in patients with temporal lobe epilepsy: an objective voxel by voxel analysis of automatically segmented MRI. J Neurol Neurosurg Psychiatry 2000;68:162–9. [PubMed: 10644781]

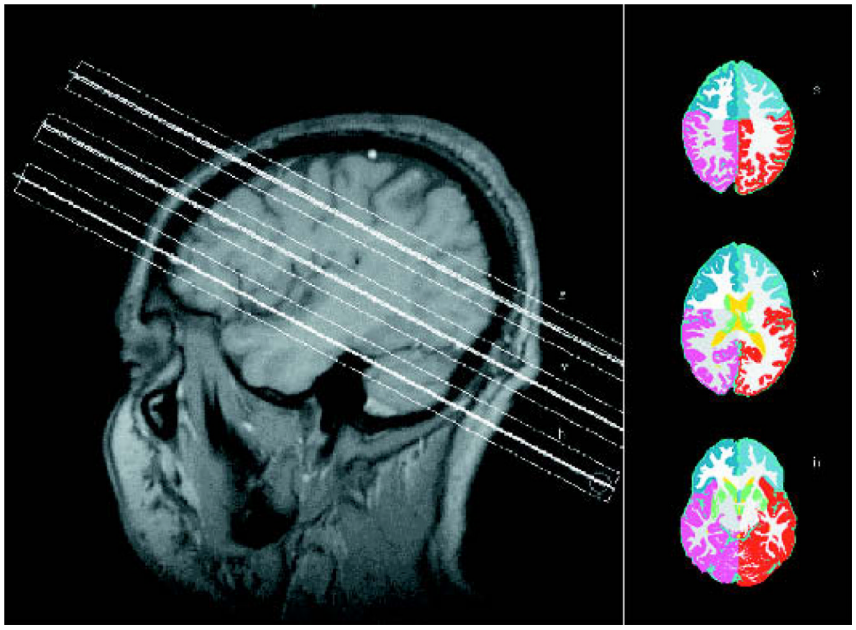

FIG. 1.

Left side: T_1-weighted sagittal image showing the position of the three slices. h, hippocampal slice; v, ventricular slice; s, supraventricular slice. **Right side:** Segmented images from the niveau of the three slices demonstrating the four regions (i.e., left and right frontal lobe and left and right nonfrontal brain). Every magnetic resonance spectroscopic imaging slice contains the information of five segmented images.

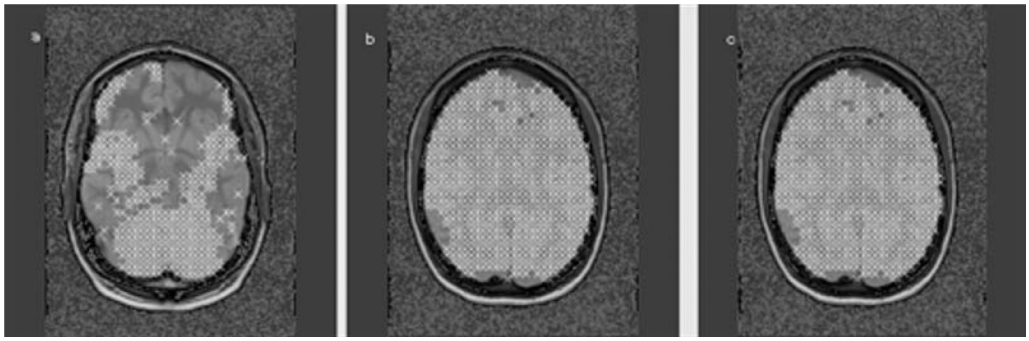

FIG. 2.

T_1-weighted axial images. The crosses represent voxels fulfilling the criteria for spectral quality as described in Methods. Whereas most of the voxels in the ventricular **(b)** and supraventricular **(c)** slice were used for regression analysis in the hippocampal slice **(a),** the voxels in the lateral temporal lobe, occipital lobe, and most of the frontal lobe had to be excluded.

TABLE 1

Patient characteristics

Patient no.	Gender/age (yr)	Years of active epilepsy	EEG	MRI	PET
1	F/53	51	Lt temp	Lt HA and incr signal	Lt temp hypo
2	M/28	8	Lt temp	Lt HA and incr signal	ND
3	M/37	30	Lt temp	Lt HA and incr signal	Lt temp hypo
4	F/45	7	Lt temp	Normal	Normal
5	F/19	7	Lt temp	Normal	Lt temp hypo
6	F/38	37	Lt temp	Lt HA and incr signal and TL atrophy	Lt temp hypo
7	M/42	28	Lt temp	Lt HA and incr signal	lt temp hypo
8	M/22	7	Lt temp	Lt HA and incr signal	ND
9	F/26	21	Lt temp	Normal	Lt temp hypo
10	F/30	1	Lt temp	Normal	Rt temp hypo
11	M/54	40	Lt temp	Lt HA	ND
12	M/43	39	Rt temp	Rt HA and incr signal	Rt temp hypo
13	F/48	40	Rt temp	Rt HA	ND
14	M/38	29	Rt temp	GM atrophy	Normal
15	M/38	17	Rt temp	Rt HA and incr signal	ND
16	M/36	35	Rt temp	Rt HA and incr signal	ND

M, male; F, female; Lt, left; Rt, right; temp, temporal; HA, hippocampal atrophy; incr signal, increased signal in hippocampal region; TL, temporal lobe; GM, gray matter; hypo, hypometabolism; ND, not done; MRI, magnetic resonance imaging; PET, positron emission tomography.

TABLE 2

Mean metabolite concentrations of left and right hemisphere combined in 100% gray and white matter in controls and patients

Region	Patients	Controls	% Difference
Frontal gray			
NAA	7.5 ± 0.91	8.1 ± 0.85	7.4[a]
Cr	3.6 ± 0.32	3.4 ± 0.45	2.1
Cho	0.9 ± 0.16	0.8 ± 0.18	1.0
Frontal white			
NAA	8.4 ± 0.96	8.9 ± 0.95	5.6
Cr	3.4 ± 0.41	3.4 ± 0.31	0
Cho	1.2 ± 0.19	1.2 ± 0.18	0
Nonfrontal gray			
NAA	8.2 ± 0.91	8.3 ± 0.83	1.2
Cr	4.6 ± 0.59	4.7 ± 0.50	2.1
Cho	1.1 ± 0.23	1.1 ± 0.17	0
Nonfrontal white			
NAA	8.6 ± 1.2	9.6 ± 1.1	10.4[a]
Cr	3.3 ± 0.34	3.3 ± 0.42	0
Cho	1.1 ± 0.15	1.1 ± 0.22	0

NAA, *N*-acetyl aspartate; Cr, creatine/phosphocreatine; Cho, choline.

[a] $p < 0.05$ when compared with controls with two-tailed signed-rank Wilcoxon test.

TABLE 3

Volume of white and gray matter as percentage of total intracranial volume

Region	Patients	Controls	% Difference
Frontal gray	Ipsi, 7.6 ± 0.87	Mean of both sides, 8.0 ± 0.51	5.0
	Contra, 7.7 ± 0.89		3.8
Frontal white	Ipsi, 5.9 ± 0.75	Mean of both sides, 5.6 ± 0.39	5.4
	Contra, 6.1 ± 0.79		8.9
Nonfrontal gray	Ipsi, 15.1 ± 0.88	Mean of both sides, 16.5 ± 0.94	8.5[a]
	contra, 15.8 ± 1.28		4.2
Nonfrontal white	Ipsi, 11.6 ± 1.1	Mean of both sides, 12.1 ± 0.48	4.9
	Contra, 12.4 ± 0.89		1.6

Ipsi, ipsilateral, l.e., hemisphere containing the epileptogenic focus; Contra, contralateral, l.e., hemisphere without epileptogenic focus.

[a] $p < 0.05$ when compared with controls with two-tailed signed-rank Wilcoxon test.